

Fabrication of uniform microlasers using conventional printing technology

Ta Van Duong^{1,†}, Hoang Thi Thuong¹, Nguyen Thanh Duy¹, Nguyen Minh Hoang² and Nguyen Van Toan³

¹*Department of Optical Devices, Le Quy Don Technical University, 236 Hoang Quoc Viet, Hanoi, Vietnam*

²*Institute of Biomedical Physics, Academy of Military Science and Technology, 109A Pasteur, Ho Chi Minh city, Vietnam*

³*Department of Physics, Le Quy Don Technical University, 236 Hoang Quoc Viet, Hanoi, Vietnam*

E-mail: [†]duong.ta@lqdtu.edu.vn

Received 28 February 2024

Accepted for publication 13 May 2024

Published 18 May 2024

Abstract. *In recent years, soft material microlasers have attracted great interest for their simple fabrication and potential in flexible photonic devices. Particularly, ink-jet printing technology offers an efficient method for the production of uniform microlasers. However, the ink-jet system is generally complex and expensive. In this work, we have successfully used a cost-effective standard printer for microlaser creation. By employing dye-doped glycerin-water for the printing ink, we can fabricate uniform dome shaped structures, the so-called hemispheres, with diameters from 35 to 70 μm on a hydrophobic coated dielectric mirror. Under optical pulse pumping at 532 nm, these hemispheres exhibit lasing emission with clear modes. The lasing mechanism is studied and ascribed to whispering gallery mode. Due to low optical loss, we achieve a lasing threshold of 32 $\mu\text{J}/\text{mm}^2$ and a quality factor of 2100. Our method can be applied to diverse soft matter microlasers and the fabricated microlasers are promising for sensing applications.*

Keywords: ink-jet printing, microlasers, standard printer, whispering gallery mode.

Classification numbers: 42.60.Da, 42.55.Mv, 42.55.Sa.

1. Introduction

Whispering gallery mode (WGM) lasers have emerged as important components in the domain of photonics [1]. These lasers exploit structures characterized by circular cross-sections, such as spheres, cylindrical fibers, disks, and rings. Through the mechanism of total internal reflection, light is effectively confined within the cavity, resulting in many advantages including minimized optical loss, compact mode volume, and a high quality (Q) factor [2]. Owing to these characteristics, WGM lasers find application across diverse fields such as optical filters, photonic integrated circuits, and highly sensitive sensors [2, 3].

Recently, soft material based WGM lasers have attracted considerable attention for their straightforward fabrication techniques and their potential integration into living cells, tissues, and flexible photonic devices [4–7]. For instance, microdroplet lasers hold promise for integration into cells to monitor internal stress levels [8]. However, achieving precise control over the size and positioning of these lasers still requires the utilization of advanced technologies such as microfluidic channels [9–11] or ink-jet printing systems [12–14]. These approaches are often characterized by complexity or high costs thus it is necessary to develop a simplified approach to produce such microlasers. The idea of employing a cost-effective standard printer has been introduced and demonstrated as an excellent solution [7] but certain adjustments are required, posing challenges for replication.

In this work, we present a cost-effective approach utilizing a standard printer (without any modification) for the production of soft-material microlasers. By replacing the traditional ink with a dye-doped glycerin-water solution, we successfully fabricate uniform dome shaped structures on a hydrophobic coated dielectric mirror. These structures exhibit contact angles of approximately 80°, very similar to hemispheres (contact angles of 90°) thus we simply refer to them as hemispheres for better visualization. The size of these hemispheres can be tuned from 35 to 70 μm . Under optical pulse excitation at 532 nm, fabricated hemispheres exhibit distinct lasing modes, with a lasing threshold of approximately 32 $\mu\text{J}/\text{mm}^2$.

2. Experiment

2.1. Preparation of printing ink

A glycerol-water mixture, with a weight ratio of 2:1, was selected as a replacement for printing ink due to its excellent compatibility with the printer. Specifically, 30 ml (approximately 45 g) of glycerol ($\geq 99\%$, sourced from Guangdong Guanghua Sci-Tech Company) was dissolved in 22.5 ml of water. Subsequently, 0.34 g of Rhodamine (RhB, 95% dye from Sigma-Aldrich) was added. The mixture was then stirred magnetically for 3 minutes to achieve homogeneity. The weight percentage of RhB in the solution is approximately 0.5%.

2.2. Preparation of hydrophobic surface

A commercial dielectric mirror ($2 \times 2 \text{ cm}^2$) was coated with a hydrophobic layer. The hydrophobic solution used was a blend of polymethylhydrosiloxane (PMHS) and tetraethylorthosilicate (TOES) in ethanol and petroleum ether solvents. After coating, the hydrophobic layer was left to dry in the air naturally for 10-15 minutes before applying another layer.

2.3. Fabrication of the hemisphere lasers

The EPSON L805 printer was utilized for the experiment. It can automatically control the positioning of the nozzles and regulate the ink ejection accordingly. The working principle is shown in Fig. 1(a). The ink is sprayed onto the hydrophobic coated dielectric mirror surface on specified coordinates. The droplets on the mirror exhibit a dome shaped structure, commonly referred to as hemispheres for simplicity.

To fabricate the hemispheres, the initial step involved loading the prepared ink solution into the cartridge of the printer. Then, Microsoft Word software was employed to perform print commands from the computer. The printed content consisted of rectangles with a size of 0.6 x 0.3 inch². The position of the rectangles was chosen to ensure they were printed accurately on the dielectric mirror placed within the CD frame as presented in Fig. 1(b). Subsequently, the print command was implemented five times repeatedly. This method can produce lasers with different sizes from about 10 to 150 μm . However, uniform sizes can not be created because the disc tray's movement causes each print to be in a different position.

To achieve uniform hemispheres, the dielectric mirror was directly placed into the printer chamber. The printed pattern comprises a dot matrix with a single dot size of 1 pt (~ 0.35 mm). When a print job is initiated, ink is sprayed onto the dielectric mirror's surface at specified coordinates, resulting in a uniform size. Interestingly, bigger droplets can be obtained by increasing the number of prints.

It is worth noting that the hydrophobic layer is important for its role in minimizing droplet adhesion to the substrate, thereby facilitating the formation of hemispheres with circular shapes through surface tension. Additionally, the dielectric mirror beneath is also significant. It is highly reflective at the emission wavelength of the dye (Fig. 1(c)) and therefore effectively reduces optical losses through the substrate, a crucial factor in achieving low-threshold lasers [15].

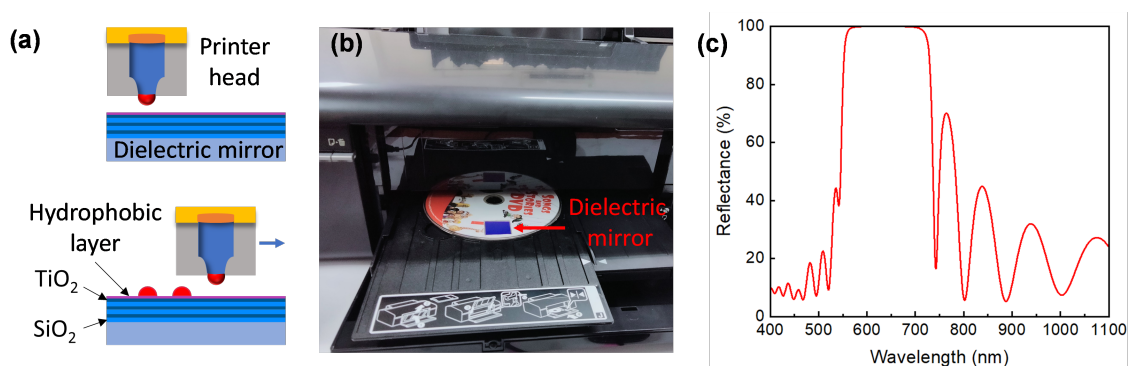


Fig. 1. (a) Schematic diagram shows the procedure of creating hemisphere microlasers using a conventional printer. (b) Image of the EPSON L805 printer with a dielectric mirror placed within the CD frame. (c) Corresponding reflectance spectrum of the dielectric mirror.

2.4. Optical characterizations

A micro-photoluminescence ($\mu - PL$) setup was employed for analyzing the dye-doped hemisphere (Fig. 2). The excitation process utilized a nanosecond pulse laser (Nd: YAG Lasers:

532 nm wavelength, 10 Hz repetition rate, 7 ns pulse duration) as the pumping source. The pumping direction was about 45° to the vertical direction. These hemisphere droplets were excited by a focused laser beam with a spot size of approximately 350 μm in diameter. Subsequently, emission from the hemisphere was collected from the top through a 10 \times objective and directed to an AvaSpec-2048L (Avantes) for spectral recording. The system's spectral resolution was approximately 0.2 nm. All optical evaluations were conducted in the air and under ambient conditions.

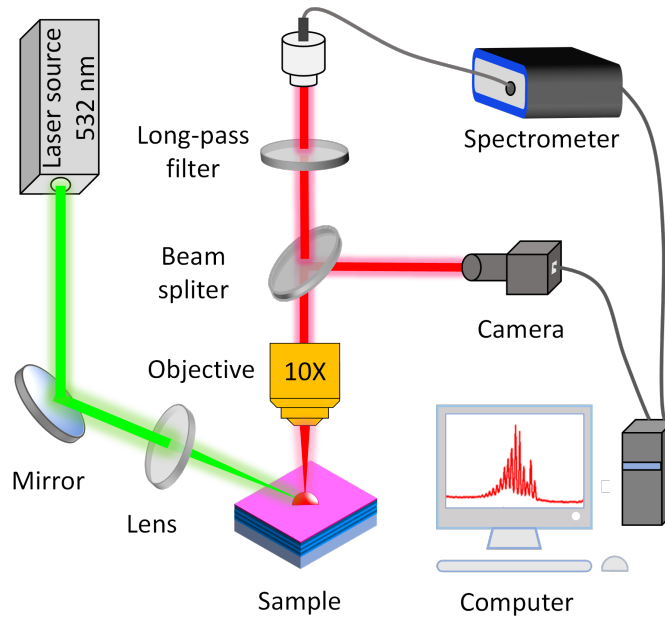


Fig. 2. Schematic of the optical setup used to study optical properties of dye-doped hemispheres.

3. Results and discussion

3.1. Microlasers with random size and position

The active material used for microlasers is RhB whose PL emission is shown in Fig. 3(a). The emission spectrum spans broadly from 530 to over 650 nm. This characteristic enables the generation of lasing emissions within a specific range.

When the dielectric mirror is placed within the CD frame, hemispheres with various sizes are obtained as shown in Fig. 3(b). These hemispheres exhibit a uniform red colour suggesting dye is well incorporated into the structure. Some microspheres appear unusually large due to multiple repeated printings, leading to overlapping and merging of microdroplets into bigger hemisphere structures.

Given the differing diameters of the hemispheres, they provide a suitable platform for studying size-dependent characteristics. Fig. 3(c) illustrates the lasing spectra of selected microlasers with diameters of 67, 83, 103, and 115 μm . In addition, microlasers of varying sizes emit laser light at different wavelengths, with the lasing envelope red shifting from 595 to 625 nm. This observation aligns with previous findings and has been well-explained [16]. In summary, the lasing

wavelength observed is strongly influenced by the efficiency of out-coupling of light (β) from the cavity to free space. β can be expressed as follows [16]:

$$\beta = \frac{Q_{\text{rad}}^{-1}}{Q_{\text{rad}}^{-1} + Q_{\text{abs}}^{-1}}, \quad (1)$$

where, Q_{rad} is the radiative quality factor, Q_{abs} is absorption loss in the cavity. It is well-known that Q_{rad} increases with the cavity size [17]. As a result, light travels a longer path inside larger hemispheres and with increased travel distance, it encounters more opportunities for reabsorption by the dye molecules. Particularly, light with shorter wavelengths is more vulnerable to reabsorption. In addition, the light at a shorter wavelength experiences more confinement within the cavity owing to increased total internal reflection. Consequently, the efficiency β increases with wavelength and lasing spectra exhibit a red shift behaviour as the size of the hemisphere increases.

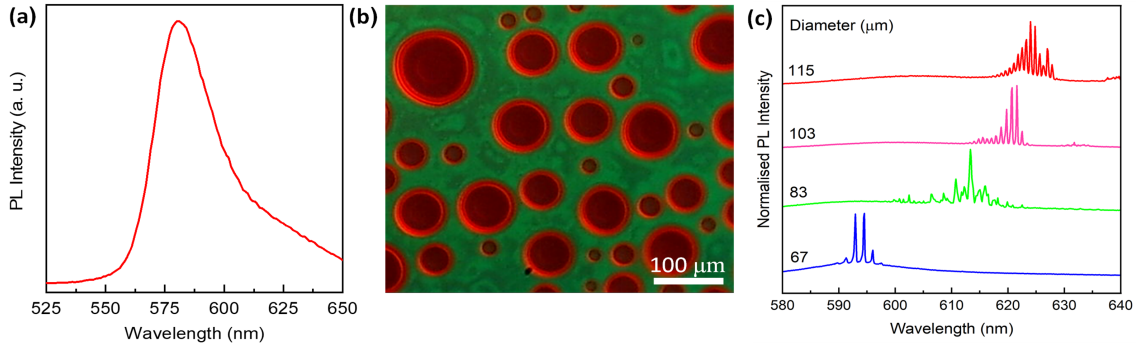


Fig. 3. (a) Microlaser emission spectrum. (b) Optical image of hemisphere microlasers with various sizes. (c) Normalized lasing spectra of hemisphere microlasers with different diameters.

3.2. Microlasers with uniform and tunable size

By directly placing the dielectric mirror into the printer chamber, we regularly obtain uniform hemispheres. Figures 4(a)-(c) depict optical microscope images of hemisphere arrays achieved through repeated printing, two, three, and five times. These hemispheres exhibit excellent alignment and uniformity in size. Specifically, when printed two, three, and five times, the hemisphere diameter measures approximately 41, 50, and 59 μm . These results confirm precise control over both the size and positioning of the hemisphere laser.

Based on the results mentioned earlier, we proceeded to print additional samples to investigate the correlation between hemisphere size and the number of printing repetitions. Fig. 4(d) illustrates the relationship between average diameter and printing repetitions. Remarkably, this graph reveals a nearly linear growth in average size with each additional printing repetition. Specifically, as the number of printings increases, the hemisphere diameter increases by about 6-8 μm after a single print. Consequently, the fundamental hemisphere size can be finely tuned within the range of 35 μm to 80 μm . Furthermore, as shown in the insets of Fig. 4(d), thanks to the hydrophobic layer, hemispheres exhibit circular shapes with a similar contact angle of 80°. These factors are favourable for whispering gallery mode resonators.

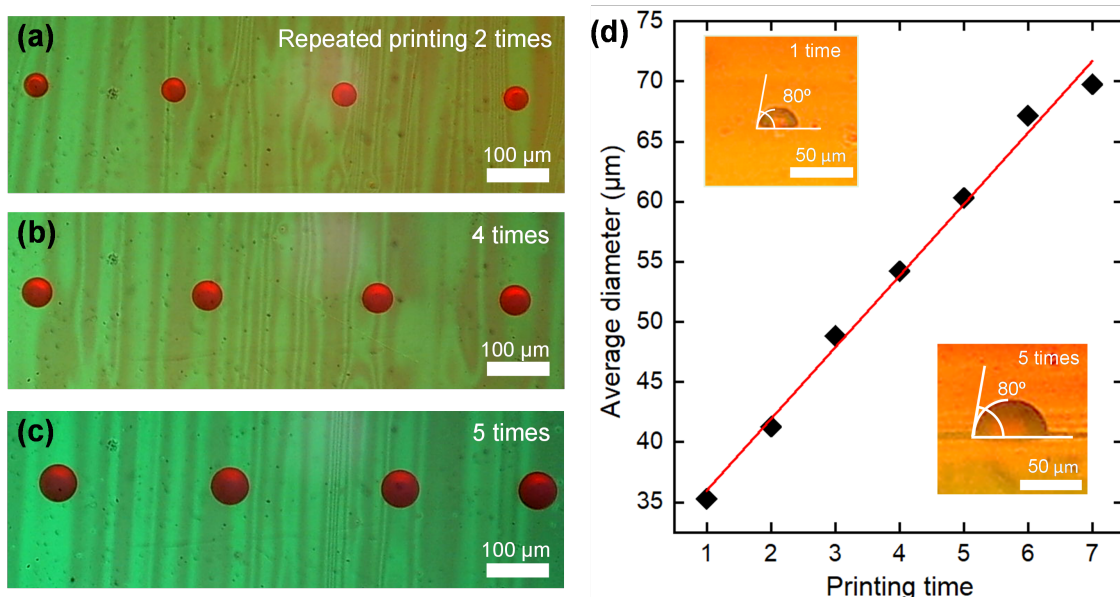


Fig. 4. (a)-(c) The optical microscope images depict the uniform hemisphere microlasers after repeated printing two, four, and five times, respectively. (d) Relationship between the average diameter of printed hemispheres and the number of repeated printings. The inset images indicate the contact angle of the hemispheres.

3.3. Lasing properties of hemisphere microlasers

Owing to their circular shape, fabricated hemispheres exhibit favourable laser emission under optical pumping. In Fig. 5(a), emission spectra of a 70 μm-diameter hemisphere are depicted indicating the evolution from spontaneous emission to lasing emission. As the pump pulse fluence (PPF) is incrementally raised, the lasing modes become evident.

At a PPF of 6.5 μJmm⁻², the emission intensity is very weak and separate modes are not observed. In principle, WGM could manifest in the fluorescent spectrum when the pump energy falls below the threshold. However, the absence of these modes may be attributed to two primary factors: (i) The efficiency of signal collection in our measurement setup has not been optimized. Since the WGM is formed in the horizontal plane thus collecting signal from the top is suboptimal. (ii) The pumping energy is suboptimal due to fluctuations in the pumping laser. Addressing these two issues could potentially enable the observation of WGM below the threshold, thereby yielding valuable insights.

Laser modes begin to emerge at 35.5 μJmm⁻² and reach very high intensity at 44 μJmm⁻². It can be also seen that the number of lasing modes also increases with the pumping fluence.

The presence of fluorescent emission within the lasing spectra is attributed to our measurement setup, which collects both fluorescent emission from the hemisphere's center and lasing emission from its edge. Nevertheless, the lasing intensity, characterized by its narrow, high-intensity peaks, significantly outweighs the broad emission of fluorescence. This observation indicates the dominance of the lasing emission in the spectra.

In addition, the PL image of the studied hemisphere shows a bright emission when PPF is above the threshold compared to that below the threshold. Interestingly, the emission is prominent along the edge, forming a distinct bright ring structure. This observation provides clear evidence of the WGM mechanism.

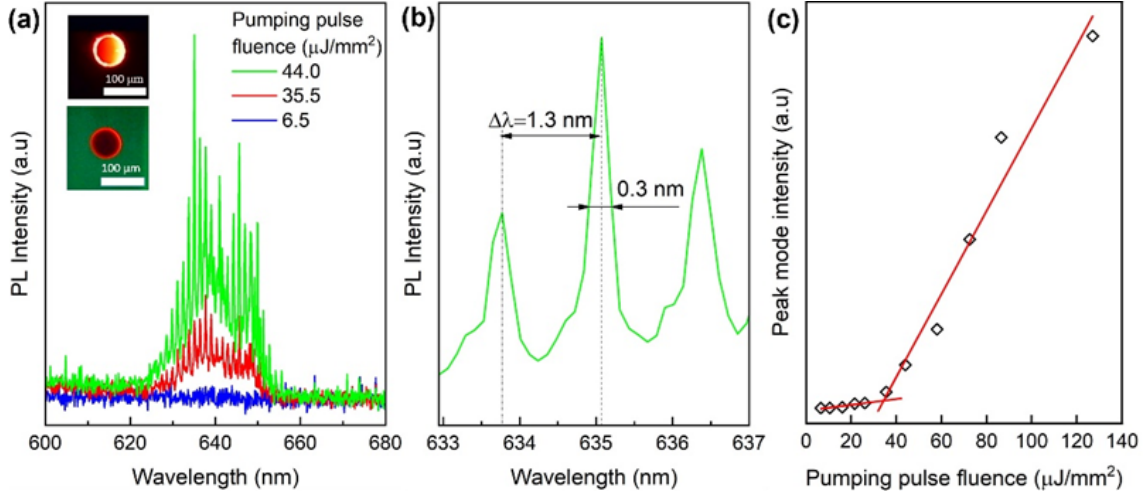


Fig. 5. (a) PL spectra of a 70 μm-diameter hemisphere laser. The inset depicts the PL image of the hemisphere under excitation below and above the lasing threshold. (b) Close-up of several lasing modes, displaying a mode spacing and a narrow spectral linewidth. (c) Peak mode intensity plotted against pump pulse fluence.

Figure 5(b) provides a close-up view of multiple lasing modes. The spectral linewidth ($\delta\lambda$) of the mode corresponding to the wavelength of 635.07 nm is 0.3 nm. This value is much narrower than the spectral linewidth of the fluorescent emission of RhB (~45 nm). In addition, the Q factor of this lasing mode can be calculated as $Q = \lambda/\delta\lambda \approx 2100$. This value is comparable to other kinds of soft matter lasers such as microsphere lasers [11] and is considered a high Q factor.

Furthermore, the mode spacing (the distance between adjacent modes, denoted as $\Delta\lambda$) can be determined to be 1.3 nm. Based on this value, we can confirm whether the lasing mechanism is due to WGM. Indeed, light travels in a closed loop along the perimeter, thus resulting in

$$m\lambda_m = \pi nD, \quad (2)$$

where m and λ_m represent the angular mode number and resonant wavelength at this mode number. D and n denote the diameter and effective refractive index of the hemisphere, respectively. From Eq. (2), the mode spacing can be derived as

$$\Delta\lambda \approx \lambda^2/(\pi nD). \quad (3)$$

Utilizing Eq. (3) while taking into account the resonant wavelength of 635 nm, a refractive index of 1.427 (calculated by Ref. [18]), and a diameter of 70 μm, the calculated mode spacing is 1.29 nm. This value is highly consistent with the measurement of 1.3 nm and therefore confirms the WGM lasing mechanism.

Based on the obtained spectra under various pumping fluences, the lasing threshold can be determined by monitoring the intensity of a typical lasing mode. Indeed, below the threshold, there is only fluorescent emission thus the peak intensity is zero. When the pumping fluence is above the threshold, peak intensity appears and increases sharply with increasing pumping fluence. As a result, the lasing threshold can be determined by plotting the mode intensity versus pumping fluence as shown in Fig. 5(c). The lasing threshold behavior can be seen clearly and it is determined to be approximately $32 \mu\text{Jmm}^{-2}$. This value is also comparable to other kinds of soft matter lasers such as droplet lasers [16].

To provide a clear visualization of the light path, a schematic view of the WGM loop within a hemisphere is presented in Fig. 6(a). Light becomes trapped inside the hemisphere in the horizontal plane due to total internal reflection at the interface between the hemisphere and the air. Moreover, the presence of a dielectric mirror underneath prevents light leakage to the substrate in the vertical plane. Consequently, light is confined in three dimensions, which is crucial for minimizing optical loss and, consequently, achieving a low lasing threshold.

To ensure that the WGM lasing mechanism is not unique to a particular hemisphere but rather universal, we conducted a study involving multiple hemispheres. Fig. 6(b) depicts the comparison between the laser mode wavelengths, as predicted by Eq. (1), and experimental measurements for three different hemispheres. The results demonstrate a consistency between theoretical predictions and experimental observations, confirming the validity of the WGM mechanism.

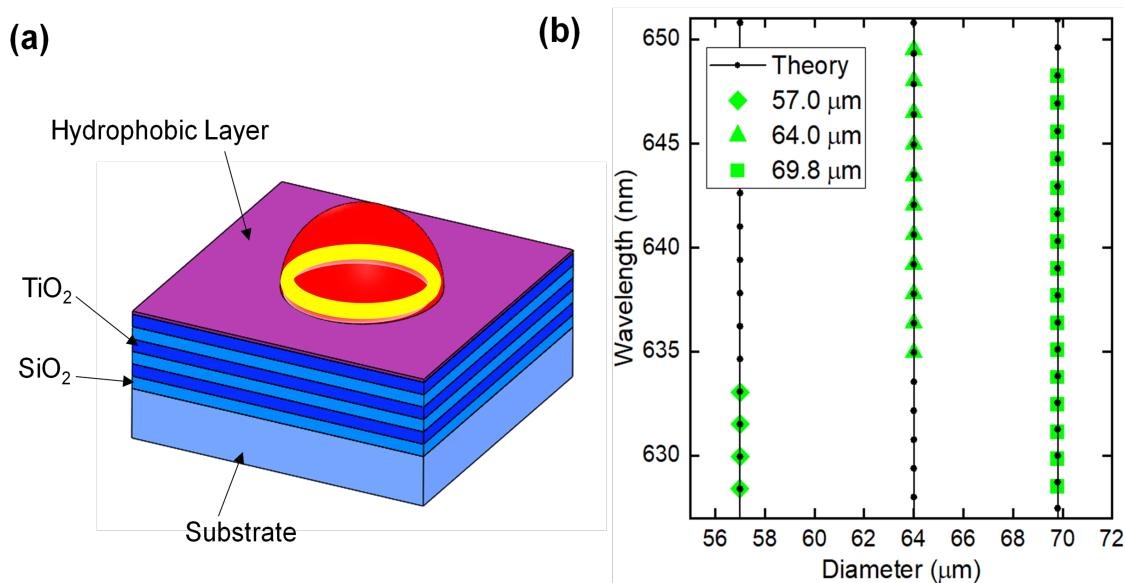


Fig. 6. (a) Three-dimensional schematic depicts a whispering gallery mode loop (yellow circle) inside a hemisphere. (b) Lasing wavelengths (represented by large symbols) compared with theoretical data (solid dots) obtained from Eq. (1).

The WGM mechanism suggests that lasing emission mainly occurs within the horizontal plane. In our setup, however, emission collection primarily occurs from the top (in the vertical

direction), indicating a suboptimal configuration. Nonetheless, lasing emission remains observable due to light scattering. As laser emission couples out of the hemisphere, a portion is directed upward. Additionally, some emission directed downward is reflected upward by the dielectric mirror. Consequently, lasing emission can be effectively captured using an optical objective. Indeed, the signal reaching the camera corresponds to that directed to the spectrometer. As a result, the presence of a bright ring in the fluorescent image of the hemisphere confirms the successful transmission of lasing emission to the spectrometer.

It is noteworthy that the hemispheres exhibit reliable performance even after being stored in a fridge for nearly a week. Due to their liquid state, there's no occurrence of cracks or structural damage on the surface. In addition, as water evaporates, the contact angle decreases. Our future investigation will go into the long-term stability of this laser, possibly extending over several weeks. However, given the simplicity and speed of the fabrication process, we prioritize using fresh samples over aged ones.

4. Conclusion

We have successfully employed a cost-efficient standard printer for the fabrication of microlasers. Utilizing dye-doped glycerin-water as the printing ink, we have achieved the production of uniform hemispheres with adjustable diameters ranging from 35 to 70 μm on a hydrophobic coated dielectric mirror. Upon optical pulse pumping, these hemispheres exhibit lasing emission characterized by well-defined modes. Through comprehensive analysis of the lasing spectrum and size-dependent characteristics, we have confirmed the underlying lasing mechanism to be attributed to the whispering gallery mode. Thanks to the low optical loss, these lasers have a low lasing threshold of 32 $\mu\text{J}/\text{mm}^2$ alongside a quality factor of 2100. Our methodology presents considerable potential for the development of soft matter microlasers across diverse applications, particularly demonstrating promise for sensing applications.

Acknowledgments

This research is funded by Vietnam National Foundation for Science and Technology Development (NAFOSTED) under grant number 103.03-2021.62.

References

- [1] S. Yang, Y. Wang and H. Sun, *Advances and prospects for whispering gallery mode microcavities*, *Adv. Opt. Mater.* **3** (2015) 1136.
- [2] J. Kerry, *Optical microcavities*, *Nature* **424** (2003) 839.
- [3] D. Yu, M. Humar, K. Meserve, R. C. Bailey, S. N. Chormaic and F. Vollmer, *Whispering-gallery-mode sensors for biological and physical sensing*, *Nat. Rev. Methods Primers* **1** (2021) 83.
- [4] V. D. Ta, Y. Wang and H. Sun, *Microlasers enabled by soft-matter technology*, *Adv. Opt. Mater.* **7** (2019) 1900057.
- [5] G.-Q. Wei, X.-D. Wang and L.-S. Liao, *Recent advances in organic whispering-gallery mode lasers*, *Laser Photonics Rev.* **14** (2020) 2000257.
- [6] D. MCGloin, *Droplet lasers: a review of current progress*, *Rep. Prog. Phys.* **80** (2017) 054402.
- [7] X. Gong, Z. Qiao, P. Guan, S. Feng, Z. Yuan, C. Huang *et al.*, *Hydrogel microlasers for versatile biomolecular analysis based on a lasing microarray*, *Adv. Photonics Res.* **1** (2020) 2000041.
- [8] M. Humar and S. H. Yun, *Intracellular microlasers*, *Nat. Photonics* **9** (2015) 572.
- [9] L.-J. Chen, L.-L. Gong, Y.-L. Lin, X.-Y. Jin, H.-Y. Li, S.-S. Li *et al.*, *Microfluidic fabrication of cholesteric liquid crystal core-shell structures toward magnetically transportable microlasers*, *Lab Chip* **16** (2016) 1206.

- [10] D. Richter, M. Marinčič and M. Humar, *Optical-resonance-assisted generation of super monodisperse microdroplets and microbeads with nanometer precision*, *Lab Chip* **20** (2020) 734.
- [11] T. Van Nguyen, T. D. Nguyen, N. Van Pham, T.-A. Nguyen and D. Van Ta, *Monodisperse and size-tunable high-quality factor microsphere biolasers*, *Opt. Lett.* **46** (2021) 2517.
- [12] V. D. Ta, S. Yang, Y. Wang, Y. Gao, T. He, R. Chen *et al.*, *Multicolor lasing prints*, *Appl. Phys. Lett.* **107** (2015) .
- [13] J. Zhao, Y. Yan, Z. Gao, Y. Du, H. Dong, J. Yao *et al.*, *Full-color laser displays based on organic printed microlaser arrays*, *Nat. Commun.* **10** (2019) 870.
- [14] R. Duan, Z. Zhang, L. Xiao, T. Ren, X. Zhou, Y. T. Thung *et al.*, *Dome-shaped mode lasing from liquid crystals for full-color lasers and high-sensitivity detection*, *Chem. Commun.* **59** (2023) 1641.
- [15] R. Chen and H. D. Sun, *Single mode lasing from hybrid hemispherical microresonators*, *Sci. Rep.* **2** (2012) 244.
- [16] S. K. Tang, R. Derda, Q. Quan, M. Lončar and G. M. Whitesides, *Continuously tunable microdroplet-laser in a microfluidic channel*, *Opt. Express* **19** (2011) 2204.
- [17] M. L. Gorodetsky, A. A. Savchenkov and V. S. Ilchenko, *Ultimate q of optical microsphere resonators*, *Opt. Lett.* **21** (1996) 453.
- [18] K. Takamura, H. Fischer and N. R. Morrow, *Physical properties of aqueous glycerol solutions*, *J. Pet. Sci. Eng.* **98** (2012) 50.